Measurement of conductive heat transfer through rarefied binary gas mixtures

Hiroki Yamaguchi[a], Jumpei Hosoi[a], Yu Matsuda[b], Tomohide Niimi[a]

[a] *Dept. of Micro-Nano Mechanical Science and Engineering, Nagoya University Furo-cho, Chikusa, Nagoya, Aichi, 464-8603 Japan.*
[b] *Dept. of Modern Mechanical Engineering, Waseda University 3-4-1, Ookubo, Shinjuku, Tokyo, 169-8555 Japan.*

Abstract

The conductive heat transfer through a rarefied binary gas mixture of helium and argon is experimentally investigated as a function of a molar fraction. The heat flux is measured from the free-molecular to near free-molecular flow regimes, and it is analyzed both in dimensional and dimensionless forms to clarify the effect from the gas-surface interaction. Then, the thermal accommodation coefficient is obtained by assuming a gas mixture as a single "virtual" species gas. The measured thermal accommodation coefficients for single component gases of helium and argon show good agreement with our previous results and data in literatures. The thermal accommodation coefficient for a binary gas mixture is compared with the theoretical value derived in the free-molecular flow regime as a superposition of an independent heat transfer by each gas component. The measured results are well explained by the theory. However, there is a little discrepancy between them, suggesting variation in the thermal accommodation coefficient with a molar fraction in flow regimes other than the free-molecular flow regime.

Key words: high Knudsen number flow, gas-surface interaction, thermal accommodation coefficient, molar fraction, heat flux

1. Introduction

The conductive heat transfer through a rarefied gas is a classical problem, and it has been studied by many researchers. In practical applications,

Email address: hiroki@nagoya-u.jp (Hiroki Yamaguchi)

gaseous mixtures are often employed, and the heat transfer through a gas mixture was studied extensively [1, 2, 3, 4, 5, 6, 7]. However, there are very few papers devoted to experimental measurements on this problem.

In a high Knudsen number flow, the number of collisions between gas and surface cannot be neglected compared with that between gas molecules. Then, gas-surface interaction is very important for understanding a thermal-fluid field in such a flow. Especially in a high Knudsen number flow of microscale, the large surface-to-volume ratio makes gas-surface interaction important. The amount of the conductive heat transfer is strongly affected by the gas-surface interaction. To represent gas-surface interactions in a practical purpose by a simple manner, an accommodation coefficient is often employed. It exhibits mean rate of exchanging a physical property between gas molecule and a surface without any detailed scattering behaviors. For a heat transfer problem, where the energy transfer between gas and surface is concerned, the energy accommodation coefficient α is employed, and it is defined by,

$$\alpha = \frac{\mathcal{E}_{\mathrm{i}} - \mathcal{E}_{\mathrm{r}}}{\mathcal{E}_{\mathrm{i}} - \mathcal{E}_{\mathrm{s}}}, \tag{1}$$

where $\mathcal{E}$ is the energy flux of incident/reflected gas molecules with the indices i for incident molecules, r for reflected molecules, and s for molecules fully accommodated to a surface. If we focus on monatomic gas species, the kinetic energy of a gas molecule is concerned. The energy accommodation coefficient is also called as the thermal accommodation coefficient.

Thermal accommodation coefficients for single gas species have been measured with various surface materials [8]. There are also several data on a gas mixture, like air. Theoretically, it sounds strange to consider the accommodation coefficient for a gas mixture, because it is defined by molecular motions. It is obtained by assuming a gas mixture as a single component "virtual" gas, namely effective value. Nonetheless, it is useful in a practical simulation, like a study on a concentrated solar power plant [9, 10]. However, the variation of a thermal accommodation coefficient as a function of the mole fraction of components in a gas mixture is not well studied experimentally. Theoretically, the thermal accommodation coefficient for gas mixture is expressed from the energy balance in the free-molecular flow regime as [11],

$$\alpha_{\mathrm{mix}} = \frac{\sum \frac{\chi_i}{\sqrt{m_i}} \alpha_i}{\sum \frac{\chi_i}{\sqrt{m_i}}}, \tag{2}$$

where α_i is the thermal accommodation coefficient, χ_i is the mole fraction and m_i is the molecular mass, of the gas component i, respectively. This expression is explained as follows: in the free-molecular flow regime, a conductive heat transfer through gas occurs by molecular motions, and the conductive heat flux q_{FM} for a single gas between two surfaces with a small temperature difference ΔT ($\ll T$) is expressed as [12, 13, 14],

$$q_{\mathrm{FM}} = \frac{\alpha}{8}\frac{\gamma+1}{\gamma-1}\frac{\bar{v}}{T}p\Delta T, \qquad \bar{v} = \sqrt{\frac{8kT}{\pi m}}, \tag{3}$$

where γ, $\bar{v}$, T, p, and m are the specific heat ratio, mean molecular speed, temperature, pressure, and molecular mass of the gas, respectively. The heat transfer for a gas mixture can be expressed by a superposition of heat transfer by each component, since there is no collision between gas molecules in gas phase in the free-molecular flow regime. Thus, the heat flux of a mixture q_{mix} is a sum of the heat flux of each component q_i with a weight of molar fraction χ_i; i.e. $q_{\mathrm{mix}} = \sum \chi_i q_i$. If components of a gas mixture has the same specific heat ratio γ, q_i is inversely proportional to the square root of the molecular mass of each component m_i, $q_i \propto 1/\sqrt{m_i}$ from Eq. (3), since T and p are common. It is important to note that the heat flux of mixture q_{mix} is calculated not from the mean molecular mass $m_{\mathrm{mix}} = \sum \chi_i m_i$ [15], but from the mean molecular speed $\bar{v}_{\mathrm{mix}} = \sum \chi_i \bar{v}_i$. Therefore, the thermal accommodation coefficient for a mixture is given by Eq. (2) for gas species with the same specific heat ratio. This theoretical equation was verified through the Nusselt number for various molar ratios of $\mathrm{H_2} - \mathrm{N_2}$ mixture by Mikami, *et al.* [11]. However, the thermal accommodation coefficient of a mixture itself is not directly analyzed as a function of molar fraction of components in detail.

Recently, we measured the viscosity slip coefficient, which is related to the tangential momentum accommodation coefficient, for a binary gas mixture at several conditions of a molar fraction [16]. From the results, the viscosity slip coefficient deviated from estimated values from numerical studies with a constant tangential momentum accommodation coefficient of each component, suggesting that the tangential momentum accommodation coefficient is a concave function of a molar fraction in a binary gas mixture. Thus, it is not so surprising that the thermal accommodation coefficient deviates from the theoretical values in flow regimes other than the free-molecular flow regime.

In this study, the conductive heat transfer through a binary gas mixture of helium and argon is experimentally measured at many conditions of a mo-

lar fraction. Then, the thermal accommodation coefficients are obtained, and they are compared with the theoretical expression, Eq. (2). Our experimental measurement system employs not only the free-molecular flow regime but also the early transitional flow regime to deduce the thermal accommodation coefficient, which is different from the theory, and the discrepancy between our results and the theoretical value is discussed.

2. Measurements

2.1. Method

The heat flux was measured between two surfaces kept at different temperatures through a rarefied gas mixture of helium and argon. The heat transfer between a spherical vacuum chamber and a flat-shaped heater kept at its center was measured as a function of pressure, and it was analyzed by assuming a concentric spherical shells geometry.

The heat transfer rate from the heater to the chamber was measured by the electrical consumption at the heater to keep its electrical resistance, namely temperature, constant. The heat transfer consists of the heat conduction through gas confined in the chamber, the radiation, and the heat conduction through the electrical leads of the heater. Only the first part depends on pressure, and the latter two parts are independent of pressure; thus, they are evaluated by the value in the vacuum limit, $p \to 0$ and are subtracted from the calculated value. The heat flux was measured in a rarefied condition, and convection was negligible.

The heat flux as a function of pressure was employed to derive the thermal accommodation coefficient at the sample surfaces. In the free-molecular flow regime, the heat flux from a heated surface at temperature T_H surrounded by a monatomic gas in a chamber at temperature T_C is expressed by Eq. (3), as previously explained. By designing the surface area ratio of T_H to T_C very small, gas molecules undergo a large number of collision to the surface at T_C before colliding to the surface at T_H, the temperature of the gas T in Eq. (3) can be approximated by T_C. Then, the accommodation coefficient α is derived from the heat fluxes measured at different pressure conditions by fitting with Eq. (3). Again, for a gas mixture, the mean molecular speed the mean molecular speed $\bar{v}_{\mathrm{mix}} = \sum \chi_i \bar{v}_i$ was used. It is important to note that the heat flux is independent of the geometrical configuration in the free-molecular flow regime.

However, as explained in our previous study [14], it is not easy to accurately measure several data points in the free-molecular flow regime, *i.e.* at a high vacuum condition, in a simplified low-cost apparatus owing to unavoidable leakage and infinitesimal heat flux to measure. Therefore, we employed a general model expression to describe the heat flux in whole flow regimes, *i.e.* from the free-molecular to continuum flow regimes. The heat flux q can be modeled by a simple empirical interpolation of the value in the free-molecular limit q_{FM}, Eq. (3), and in the continuum limit, q_C, as in Refs. [13, 14, 17, 18, 19, 20], and it is expressed as

$$\frac{1}{q} = \frac{1}{q_{FM}} + \frac{1}{q_C}. \tag{4}$$

Recently, we analyzed the heat transfer in our measurement system [21], and we found that our system was well explained by a concentric spherical shells geometry. However, the heat flux started to deviate in high pressure conditions, and we proposed a revised empirical function for better fitting using numerical results by the S-model kinetic equation. Unfortunately, the revised function was derived only from the results of pure gases, helium, argon and xenon, and there is no reason for the function to be applicable to a gas mixture. Thus, we used the original form, Eq. (4), employed in our previous experimental studies [14, 13]. Meanwhile, pressure conditions were limited below 1.4Pa in the measurement to ensure the near free-molecular flow regime, so that the effect from the value in the continuum limit was minimized.

To use Eq. (4) for the fitting to obtain the accommodation coefficient, the heat flux in the continuum limit q_C is needed. The heat flux in the continuum limit q_C is described by Fourier's law, and it is independent of pressure but dependent on the geometrical configuration of two surfaces at different temperatures. Therefore, the geometry of a measurement system is better to be symmetry, and we design our system in the concentric spherical shells geometry. Considering that a sample with a flat surface is much easy to prepare, the flat-plate shaped heater with sample substrates is employed instead of an inner spherical shell. By making the size of the heater much smaller than the external spherical shell, *i.e.* the spherical vacuum chamber, the heat transfer problem between the heater and the chamber can be approximated by the problem in the concentric spherical shells geometry [21, 14]. The equivalent radius of the inner spherical shell calculated from a sphere having the same surface area with the heated surfaces was obtained as $R_H = 4.95$mm. The

radius ratio of the concentric spherical shells geometry, $\mathcal{R} = R_C/R_H$, was equal to 10. By assuming the geometry, the theoretical heat flux in the continuum limit q_C could be obtained. The temperature distribution and the temperature dependence of the thermal conductivity in the continuum limit are considered following our recent analysis [21]. The temperature variation from the conductive heat transfer between two concentric spherical shells in radius direction r is described from the energy balance for a static fluid as,

$$\frac{\partial}{\partial r}\left(r^2\kappa(T)\frac{\partial T}{\partial r}\right) = 0, \tag{5}$$

where $\kappa(T)$ is the thermal conductivity of the gas, which is a function of temperature. The heat flux is calculated by the Fourier's law as,

$$q = -\kappa(T)\frac{dT}{dr}. \tag{6}$$

The thermal conductivity $\kappa(T)$ was assumed to be proportional to T^{ω_T} in this study, which is similar to the model by using the inverse power law potential for a monatomic single gas, like the Variable Hard Sphere (VHS) model [22]. ω_T is named as the thermal conductivity index hereafter. Since the temperature of the gas in the vicinity of a wall is equal to that of the wall in the continuum limit, Eqs. (5) and (6) are solved analytically, and the heat flux from the heated inner spherical shell becomes [21],

$$q_C = \kappa(T_C)\frac{\mathcal{T}^{\omega_T+1}-1}{(\omega_T+1)(\mathcal{T}-1)}\left(T_H - T_C\right)\frac{R_C R_H}{R_C - R_H}\frac{1}{R_H^2}. \tag{7}$$

where $\mathcal{T}$ is the temperature ratio $\mathcal{T} = T_H/T_C$. The difference from the constant thermal conductivity case in our previous studies [14, 13] is that the heat flux is multiplied by a factor $\left(\mathcal{T}^{\omega_T+1}-1\right)/\left\{(\omega_T+1)(\mathcal{T}-1)\right\}$.

The thermal conductivity of pure gas components, helium and argon, is determined by fitting the data in Ref. [23] by,

$$\kappa(T) = \kappa_{\mathrm{ref}}\left(\frac{T}{T_{\mathrm{ref}}}\right)^{\omega_T}, \tag{8}$$

where κ_{ref} is a reference value at temperature T_{ref}. The reference temperature was chosen to be close to T_C. The thermal conductivity index ω_T was obtained from the gradient of a log-log plot of the thermal conductivity as a

Table 1: The reference thermal conductivity κ_{ref} at a reference temperature $T_{\mathrm{ref}} = 300\mathrm{K}$ and the thermal conductivity index ω_T for He-Ar binary gas mixture at every 10% of molar fractions.

He	Ar	κ_{ref} (mW/(m · K))	ω_T
0%	100%	17.84	0.8218
10%	90%	23.80	0.8064
20%	80%	30.57	0.7945
30%	70%	38.33	0.7842
40%	60%	47.30	0.7745
50%	50%	57.80	0.7648
60%	40%	70.23	0.7544
70%	30%	85.21	0.7428
80%	20%	103.6	0.7293
90%	10%	126.5	0.7130
100%	0%	156.0	0.6923

function of temperature. κ_{ref} at $T_{\mathrm{ref}} = 300\mathrm{K}$ and ω_T were $156.0\mathrm{mW/(m \cdot K)}$ and 0.6923 for helium and $17.84\mathrm{mW/(m \cdot K)}$ and 0.8218 for argon, respectively. To express the thermal conductivity for a gas mixture, the expression by Mason and Saxena [24] was employed from the value for each component as,

$$\kappa_{mix} = \frac{\kappa_1}{1 + A_{12}\frac{\chi_2}{\chi_1}} + \frac{\kappa_2}{1 + A_{21}\frac{\chi_1}{\chi_2}}, \qquad A_{ij} = 1.065\frac{\left[1 + \left(\frac{\kappa_i}{\kappa_j}\right)^{\frac{1}{2}}\left(\frac{M_i}{M_j}\right)^{\frac{1}{4}}\right]^2}{\left[8\left(1 + \frac{M_i}{M_j}\right)\right]^{\frac{1}{2}}}, \quad (9)$$

where χ_i, M_i is the molar fraction and molecular weight of i component, respectively. The molar fraction was varied every 10%, and the obtained reference thermal conductivities and thermal conductivity indexes for the binary gas mixture are listed in Table 1. Although the effect of the continuum limit was reduced by limiting pressure range, the effect from the thermal conductivity is evaluated by using values obtained from recent *ab initio* simulations [25, 26, 27] and values in 1984 [28], which are available only for limited molar ratio conditions.

2.2. Setup

The experimental setup is explained in detail elsewhere [14].

A spherical vacuum chamber made by Pyrex has the inner radius of $R_C = 49.5$mm. It was immersed in a water bath at a room temperature to keep the temperature T_C constant. The pressure, which was assumed to be uniform inside the chamber, was measured by a temperature-controlled capacitance manometer (MKS, Baratron ®627B) directly connected to the chamber.

A tiny flat-shaped heater of $11.8 \times 12 \times 0.38$ mm^3 designed for this system (Toyo Precision Parts MFG) was placed at the center of the spherical vacuum chamber. Two thin sample substrates were placed on both sides of the heater. For a surface material, platinum was selected, since there are many data and our previous measurements to check the validity of this measurement. A platinum foil with a thickness of 10 μm (Nilaco) was employed. The heater was maintained at temperature T_H by an analog electrical bridge circuit, and the heat transfer rate from the heater was calculated from the voltage and current of the heater.

The test gas of a binary gas mixture was prepared by using a gas mixing system (Alicat Scientific, Flow Vision MX ™) with mass flow controllers (Alicat Scientific, MCV-100SCCM-D) from pure gas components of helium and argon prepared by commercially available gas cylinders.

3. Results and Discussion

3.1. Heat flux through binary gas mixture

The heat fluxes were measured three times by varying the pressure condition for each molar ratio. The measured heat fluxes as a function of pressure are plotted in Fig. 1 (a). To show the scatterings of data as an indication of the measurement accuracy, all the measured heat flux are plotted. From the figure, the plots show similar profiles for all molar ratio conditions, and they increase almost linearly. However, if we focus on the results as a function of molar fraction, they are in a complicated order.

To make the problem simple and to be comparable to theoretical studies, the heat flux was evaluated in a dimensionless form. Following the previous studies [4, 29, 21], the rarefaction parameter δ_0, which is inversely proportional to the Knudsen number, is defined as,

$$\delta_0 = \frac{R_0}{l}, l = \frac{\mu(T_0)v_0}{p}, v_0 = \sqrt{\frac{2kT_0}{m_0}}. \tag{10}$$

Here $R_0 = R_C - R_H$ is the characteristic length, l_0 is the equivalent mean free path, p is pressure inside the chamber, $\mu(T_0)$ and v_0 are the viscosity and the

most probable molecular speed at the reference temperature T_0, respectively. The reference temperature T_0 is taken as $T_0 = T_C$. The viscosity for a mixture is calculated from the data for pure gases [23] by the Wilke's method. The discrepancies of δ_0 for a mixture (He 50%:Ar 50%) from that calculated with the viscosity obtained by using *ab initio* intermolecular potentials [27] were less than 3.4%. The reference molecular mass m_0 was calculated by the mean molecular mass of the mixture as,

$$m_0 = \chi_1 m_1 + \chi_2 m_2, \chi_1 + \chi_2 = 1. \tag{11}$$

The heat flux q is related to the dimensionless form q^* as,

$$q = q^* \cdot p v_0 \frac{\Delta T}{T_0}, \tag{12}$$

where $\Delta T = T_H - T_C$.

The dimensionless heat fluxes q^* are plotted in Fig. 1 (b). In the free-molecular flow regime, the dimensionless form q^* becomes independent of the rarefaction parameter δ_0. Therefore, a flat region of the plots is an indication of the free-molecular flow regime. For all molar ratio conditions, the plots are almost flat and start to decrease at $\delta_0 > 1$, validating that the heat fluxes were measured from the free-molecular to near free-molecular flow regimes. The heat flux monotonically decreases with increase in the molar fraction of helium. In the numerical study using *ab initio* intermolecular potentials [5], the heat fluxes for pure components of helium and argon are reported as almost the same for whole range of the rarefaction parameter δ_0; while experimentally, they varies largely with the molar ratio. It is indicated that the variation with the molar ratio is due to a large variation in the thermal accommodation coefficient. Therefore, it is important to understand the gas-surface interaction to compare with the results in literatures. Relatively large scatterings of the plots in the small δ_0 region is due to the difficulty in measuring small heat transfer rates.

3.2. Thermal accommodation coefficient for pure gas species

Surface substrates of platinum were renewed from our previous measurement [14]. Thus, we measured the thermal accommodation coefficient for pure helium and argon to validate the values of this study by comparing them with our previous study and other studies. The thermal accommodation coefficient was measured three times for each gas species to check the repeatability of the measurement.

Table 2: The dimensional heat fluxes q as a function of pressure p for He 0%:Ar 100%, He 50%:Ar 50% and He 100%:Ar 0% are tabulated.

He 0%:Ar 100%		He 50%:Ar 50%		He 100%:Ar 0%	
p (Pa)	q (W/m^2)	p (Pa)	q (W/m^2)	p (Pa)	q (W/m^2)
0.0125	0.315	0.00943	0.205	0.0135	0.359
0.0141	0.341	0.0126	0.239	0.0144	0.406
0.0148	0.362	0.0155	0.332	0.0153	0.414
0.0542	1.46	0.0537	1.21	0.0525	1.63
0.0556	1.39	0.0564	1.31	0.0530	1.59
0.0558	1.53	0.0593	1.31	0.0554	1.60
0.105	2.77	0.106	2.26	0.102	2.91
0.106	2.63	0.109	2.45	0.103	3.04
0.110	2.87	0.111	2.44	0.108	3.10
0.207	5.36	0.211	4.70	0.206	5.84
0.210	5.23	0.212	4.70	0.208	6.05
0.217	5.76	0.213	4.67	0.209	5.86
0.305	7.46	0.312	6.76	0.303	8.71
0.313	7.86	0.316	6.94	0.307	8.67
0.318	8.30	0.319	7.11	0.309	8.74
0.418	10.7	0.413	8.90	0.400	11.4
0.419	10.2	0.421	9.12	0.406	11.4
0.419	10.3	0.422	9.25	0.413	11.5
0.622	15.6	0.614	13.0	0.619	17.1
0.622	15.5	0.620	13.0	0.619	17.5
0.629	14.9	0.621	13.3	0.622	17.4
0.820	19.9	0.809	17.0	0.798	22.1
0.820	20.0	0.817	17.0	0.817	23.0
0.827	19.1	0.827	17.0	0.821	22.8
1.03	24.3	1.02	20.8	1.03	28.4
1.03	24.4	1.03	21.2	1.03	28.9
1.03	23.3	1.03	20.9	1.04	28.6
1.23	28.3	1.21	24.2	1.22	33.9
1.23	28.5	1.23	24.7	1.23	34.6
1.23	27.2	1.23	25.0	1.24	34.1

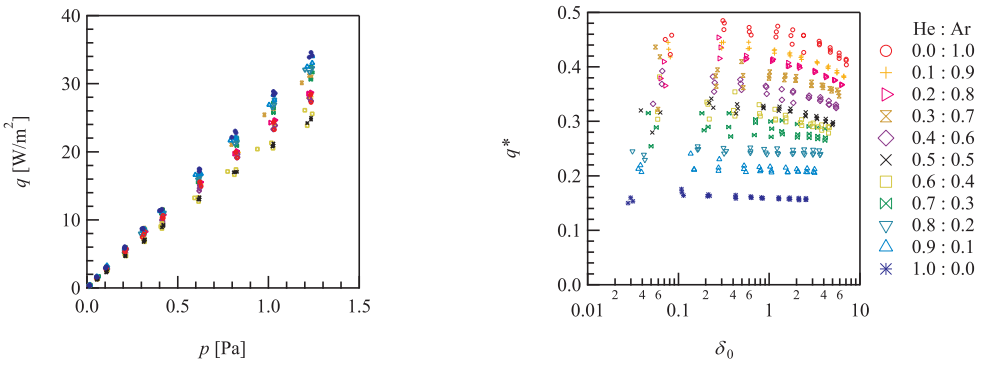

(a) dimensional (b) dimensionless

Figure 1: (Color online) All of the measured heat fluxes as a function of pressure for binary gas mixtures every 10% are plotted; (a) dimensional and (b) dimensionless forms.

The hot surface temperature T_H is approximately 340K and the cold surface temperature T_C is at a room temperature, and they are almost constant. The measured heat flux is fitted by Eq. (4) with Eqs. (3) and (7), whose expression in the continuum limit is corrected [21] from the previous measurement [14]. This correction considers the temperature distribution inside the chamber; while it was assumed to be uniform at T_C in the original analysis. In this study, by applying this correction, the obtained thermal accommodation coefficient reduced from the original analysis by less than 0.1% for helium and 0.9% for argon. Therefore, this revision does not affect the result so much.

The results of the thermal accommodation coefficient on the platinum foil surface are plotted in Fig. 2. Three data points obtained in this study are plotted in the figure. It is difficult to distinguish each other especially in helium, Fig. 2 (a), because three measured values are aggregated in a single value, showing good repeatability of the measurement system. From the figure, measured thermal accommodation coefficients show good agreement with other data in literatures [18, 13, 30, 31]. In addition to that, measured values in this study give nearly the same with that in our previous study [21], showing good reproducibility. The reason for a little scattered data in argon could be cleanliness of the surface sample, where the time under vacuum before a measurement is not so long in this study. However, the discrepancy is negligibly small compared with scattering of data in literatures.

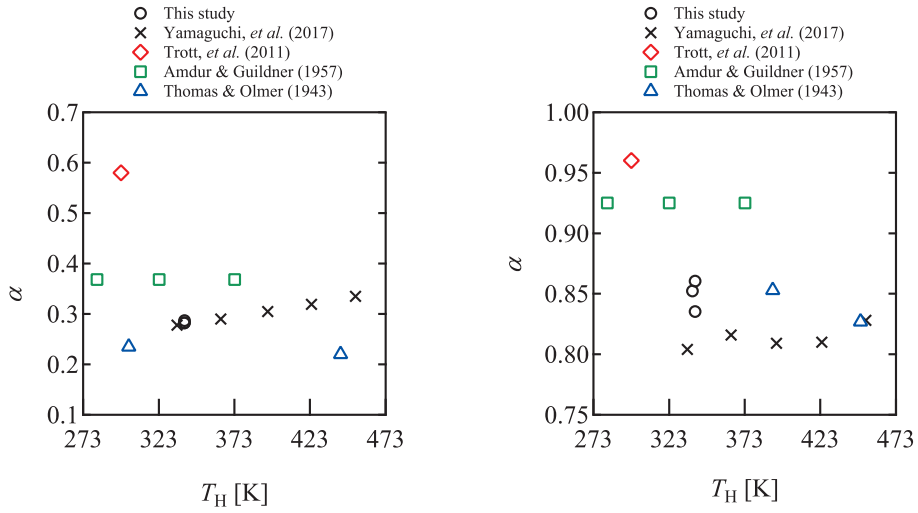

(a) He (b) Ar

Figure 2: (Color online) The measured thermal accommodation coefficients on platinum for three measurements are plotted for pure gas species; (a) helium and (b) argon, and compared with published data in literatures [18, 30, 31].

3.3. Thermal accommodation coefficient for binary gas mixture

To obtain the thermal accommodation coefficient for a binary gas mixture, the measured heat flux is also fitted by Eq. (4). It is re-emphasized that the heat flux of a gas mixture in Eq. (3) is calculated from the mean molecular speed, $\bar{v}_{\rm mix} = \sum \chi_i \bar{v}_i$. The heat flux was measured three times at each molar fraction, and the obtained thermal accommodation coefficients were averaged.

The results are shown in Fig. 3 and Table 3. Temperature conditions are also listed in the table.

To verify the use of Eq. (9) for the thermal conductivity of gas mixtures on calculating q_C in the continuum limit, the thermal accommodation coefficients are also obtained by using the thermal conductivity by *ab initio* simulations [25, 26, 27] and by Kestin, *et al.* (1984) [28] for the available molar ratio conditions. The results are plotted in Fig. 3 and Table 3. The discrepancies are very small, which is reasonable by considering that the heat flux was measured in the near free-molecular flow regime. Thus, it is reasonable to use Eq. (9) for the the thermal conductivity.

To compare the results with the theoretical value in the free-molecular

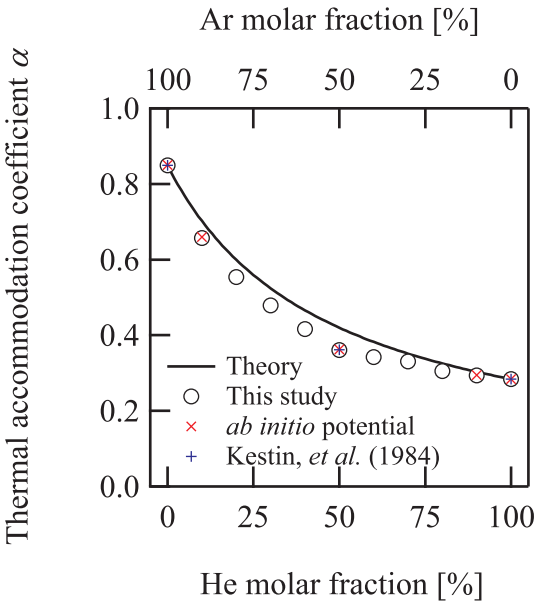

Figure 3: The measured thermal accommodation coefficients as a function of a molar fraction are plotted by markers. The thermal conductivity is changed for the calculation of q_C to the value obtained from *ab initio* simulations [25, 26, 27] and by Kestin, *et al.* (1984) [28]. They are compared with the theoretical curve calculated by Eq. (2) using thermal accommodation coefficients of each component obtained in this study.

flow regime, Eq. (2), a curve is calculated by using the thermal accommodation coefficients for pure gas components, helium and argon, measured in this study, which is also plotted in the figure. Since the theoretical curve for the binary gas mixture is calculated from the measured values for helium and argon, data points of helium 0% (argon 100%) and helium 100% (argon 0%) are exactly on the curve. The data points are almost explained by the theoretical concave curve. This slightly curved tendency connecting two thermal accommodation coefficients of pure gas components is also obtained by a molecular dynamics study using the pair of argon - xenon (Fig. 7 in [15]). Thus, it is reasonable to use the theoretical relation to evaluate the thermal accommodation coefficient for a binary gas mixture.

The dimensionless heat flux q^* monotonically decrease with increasing in the fraction of helium in a gas mixture in Fig. 1 (b), which is considered to be the effect of the gas-surface interaction. By using the obtained thermal

Table 3: The measured thermal accommodation coefficients with temperature conditions. The thermal conductivity is changed for the calculation of q_C to the value obtained from *ab initio* simulations [25, 26, 27] and by Kestin, *et al.* (1984) [28].

He	Ar	T_H[K]	T_C[K]	α	*ab initio*	Kestin, *et al.*
0%	100%	339.6	293.1	0.8492	0.8500	0.8492
10%	90%	340.6	293.0	0.6571	0.6594	
20%	80%	339.9	291.8	0.5535		
30%	70%	344.7	293.1	0.4788		
40%	60%	338.6	292.7	0.4165		
50%	50%	334.2	292.1	0.3610	0.3620	0.3619
60%	40%	333.8	292.7	0.3419		
70%	30%	340.5	292.9	0.3304		
80%	20%	339.9	291.9	0.3047		
90%	10%	339.6	292.3	0.2940	0.2942	
100%	0%	340.0	293.1	0.2838	0.2837	0.2837

accommodation coefficients, the measured heat fluxes are compared with the numerical results in literatures [5, 21]. In the free-molecular flow regime, the heat flux is proportional to the thermal accommodation coefficient as in Eq. (3). Thus, the dimensionless heat flux q^* is divided by the thermal accommodation coefficient α to exclude the effect from the gas-surface interaction for direct comparison. q^*/α are plotted in Fig. 4 (a). It is worth noting that the geometrical configuration is the parallel plates in Ref. [5], whereas the concentric spheres are employed in Ref. [21]. The characteristic length R_0 is the distance between the surfaces. From the figure, the results of helium and argon give almost the same values including the experimental results. Therefore, it is verified that the variation of the dimensionless heat flux in Fig. 1 (b) results from the gas-surface interaction. In the free-molecular flow regime with small δ_0, all of the results show quite good agreement. However, the numerical results of the parallel plates start to decrease much smaller δ_0 condition. This could be because of the difference in the geometrical configuration. Therefore, the characteristic length is changed to $R_0 = R_H$ in Fig. 4 (b). The curves show good agreements; while, there is a small discrepancy in large δ_0 region, indicating the difference in the geometrical configuration still remains. The heat flux is also compared with the result of a gas mixture (He 50%:Ar 50%) in Ref. [5]. From the figure, the reasonable agreements are observed even for the results of the gas mixture, and it is validated that the

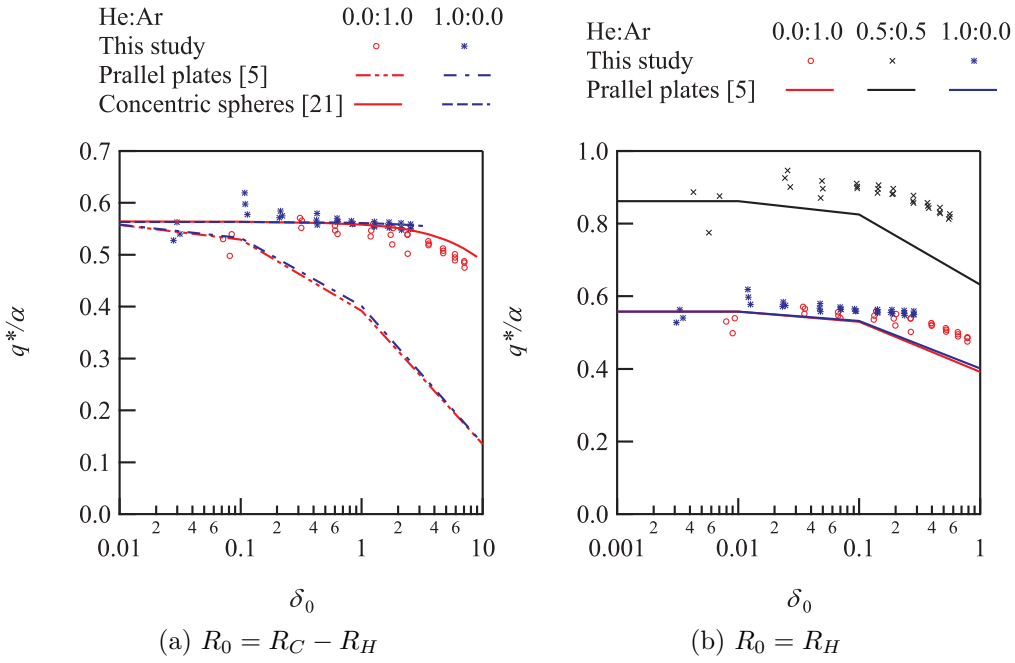

(a) $R_0 = R_C - R_H$ (b) $R_0 = R_H$

Figure 4: (Color online) The dimensionless heat flux divided by the obtained thermal accommodation coefficient is plotted for pure pure gas species and a gas mixture (He 50%:Ar 50%), and compared with published data in literatures for the parallel plates geometry [5] and for the concentric spheres geometry [21]; (a) the characteristic length $R_0 = R_C - R_H$ and (b) $R_0 = R_H$.

dimensionless heat flux for the mixture is larger than that for a single gas.

However, if we investigate Fig. 3 carefully, there is a small discrepancy between the plots and curve. It is interesting to point out that all the plots lie below the curve, even though there is a scattering of data due to a measurement error. The plots of pure gas components, which are at both ends of the curve, also suffer from the measurement error as well as the plots for gas mixtures between them; nevertheless, all the plots deviate in the same side, smaller than the curve. Therefore, it is natural to consider that the smaller thermal accommodation coefficients are owing to the mixing of two gas components, the nature of gas mixture. In addition to that, the thermal accommodation coefficient showed about 5% reduction in maximum by the revision of the empirical function, Eq. (4), in our recent study [21]. Therefore, even by the revision of the empirical function to derive the thermal

accommodation coefficient, the thermal accommodation coefficient will decrease, resulting in enlarging the discrepancy from the curve. In our previous study [16], the viscous slip coefficient was measured for a binary gas mixture as a function of a molar fraction. The viscous slip coefficient was a convex function of a molar fraction, whose shape was similar to that obtained by numerical simulations qualitatively; however, there were discrepancies quantitatively. It was considered that the difference in the tangential momentum accommodation coefficients for pure gas components between our measurement and the numerical studies resulted in the discrepancies. However, it was difficult to explain our measured results from an extrapolation of the numerical results only by the difference in values for pure gas components, and it was necessary to assume the accommodation coefficient as a function of a molar fraction for fitting our results by the numerical results. The tangential momentum accommodation coefficient was estimated as a concave function of a molar fraction. From this result, the accommodation coefficient in the slip flow regime was implied to vary with a molar fraction. Since the thermal accommodation coefficient measured in this study was analyzed from the data not only in the free-molecular but also in the early transitional flow regime, it is not strange to assume that our measured thermal accommodation coefficients suffer from this characteristics. Thus, the ratio of the measured thermal accommodation coefficient to the theoretical one is calculated and plotted in Fig. 5. The error bar is calculated from the standard error for three measurements. The detailed assessment of uncertainties could be realized by the uncertainty quantification technique [32]. From the figure, a concave tendency of the thermal accommodation coefficient can be observed. Just for an indication of tendency, a quadratic function, $y = 1 + Ax(1 - x)$, which gives unity at both ends of 0% and 100% in the molar fraction, is also plotted by a dashed line, where A is a constant and x is the molar fraction. It is important to note that the ratio is almost unity and the smallest value is even larger than 0.85. From the accuracy of our simplified measurement system, the only conclusion is that the measured thermal accommodation coefficient was almost the same with the theoretical one; however, it is suggested that the thermal accommodation coefficient decreases by mixing two gas components in the slip flow regime. There is, of course, a possibility of the effect of the empirical relation used in this study, since it did not fit well to the numerical results by the S-model kinetic equation [21]. Therefore, the measurements of the temperature jump coefficient for a binary gas mixture is needed [33], which will reveal this characteristics directly.

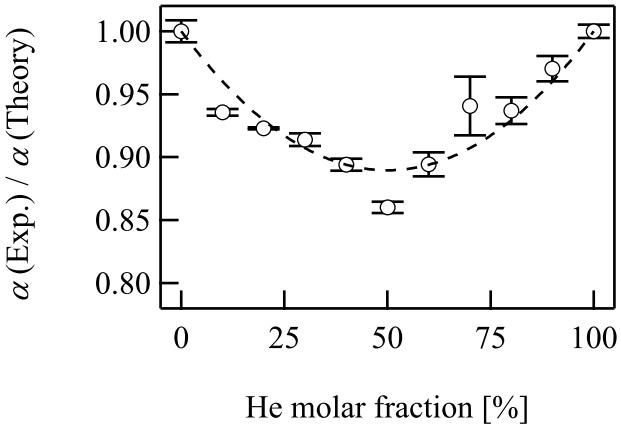

Figure 5: The ratio of the measured thermal accommodation coefficient to the theoretical value obtained by Eq. (2) are plotted by markers. Dashed line is a quadratic function $y = 1 + Ax(1 - x)$ just for an indication of the shape. Error bars indicate the standard errors.

4. Conclusions

The conductive heat flux through a rarefied binary gas mixture of helium and argon is measured as a function of molar fraction every 10%. The dimensionless heat flux monotonically decreases with increasing the molar fraction of helium. This is coming from the large difference in the thermal accommodation coefficient between helium and argon.

Then, the thermal accommodation coefficients were obtained for binary gas mixtures. The measured thermal accommodation coefficients for pure gas components showed good agreements with our previously reported values and data in literatures, showing good repeatability and reproducibility of our measurement system. For a binary gas mixture, the measured thermal accommodation coefficient was well explained by the theoretical curve derived by considering a superposition of an independent heat transfer by each gas component in the free-molecular flow regime.

If we investigate the results carefully, the thermal accommodation coefficient was below the theoretical curve, inferring a concave variation of the coefficient as a function of a molar fraction. This characteristics would be similar to those observed in the viscous slip coefficient for a binary gas mixture.

Acknowledgments

This research was partially supported by MEXT/JSPS KAKENHI Grant Number 16K14157 and 18K03946.

References

[1] S. Kosuge, K. Aoki, and S. Takata. Heat transfer in a gas mixture between two parallel plates: Finite-difference analysis of the boltzmann equation. *AIP Conference Proceedings*, 585(1):289–296, 2001.

[2] R. D. M. Garcia and C. E. Siewert. The mccormack model for gas mixtures: Heat transfer in a plane channel. *Phys. Fluids*, 16(9):3393–3402, 2004.

[3] R. D. M. Garcia and C. E. Siewert. Heat transfer between parallel plates: An approach based on the linearized boltzmann equation for a binary mixture of rigid-sphere gases. *Phys. Fluids*, 19(2):027102, 2007.

[4] F. Sharipov, L. M. G. Cumin, and D. Kalempa. Heat flux between parallel plates through a binary gaseous mixture over the whole range of the knudsen number. *Physica A*, 378(2):183 – 193, 2007.

[5] J. L. Strapasson and F. Sharipov. Ab initio simulation of heat transfer through a mixture of rarefied gases. *Int. J. Heat Mass Transf.*, 71:91 – 97, 2014.

[6] M. T. Ho, L. Wu, I. Graur, Y. Zhang, and J. M. Reese. Comparative study of the boltzmann and mccormack equations for couette and fourier flows of binary gaseous mixtures. *Int. J. Heat Mass Transf.*, 96:29 – 41, 2016.

[7] C. Tantos and D. Valougeorgis. Conductive heat transfer in rarefied binary gas mixtures confined between parallel plates based on kinetic modeling. *Int. J. Heat Mass Transf.*, 117:846 – 860, 2018.

[8] S. C. Saxena and R. K. Joshi. *Thermal Accommodation and Adsorption Coefficients of Gases*. Hemisphere, New York, 1981.

[9] R. Vinuesa, L. Fdez. de Arevalo, M. Luna, and H. Cachafeiro. Simulations and experiments of heat loss from a parabolic trough absorber tube over a range of pressures and gas compositions in the vacuum chamber. *J. Renewable Sustainable Energy*, 8(2):023701, 2016.

[10] H. Cachafeiro, L. Fdez. de Arevalo, R. Vinuesa, J. Goikoetxea, and J. Barriga. Impact of solar selective coating ageing on energy cost. *Energy Procedia*, 69:299–309, 2015.

[11] H. Mikami, Y. Endo, and Y. Takashima. Heat transfer from a sphere to rarefied gas mixtures. *Int. J. Heat Mass Transf.*, 9:1435–1448, 1966.

[12] E. H. Kennard. *Kinetic Theory of Gases*. Hemisphere, New York, 1938.

[13] H. Yamaguchi, K. Kanazawa, Y. Matsuda, T. Niimi, A. Polikarpov, and I. Graur. Investigation on heat transfer between two coaxial cylinders for measurement of thermal accommodation coefficient. *Phys. Fluids*, 24(6):062002, 2012.

[14] H. Yamaguchi, T. Imai, T. Iwai, A. Kondo, Y. Matsuda, and T. Niimi. Measurement of thermal accommodation coefficients using a simplified system in a concentric sphere shells configuration. *J. Vac. Sci. Technol. A*, 32(6):061602, 2014.

[15] S. K. Prabha and S. P. Sathian. Determination of accommodation coefficients of a gas mixture in a nanochannel with molecular dynamics. *Microfluid. Nanofluid.*, 13:883–890, 2012.

[16] H. Yamaguchi, K. Takamori, P. Perrier, I. Graur, Y. Matsuda, and T. Niimi. Viscous slip coefficients for binary gas mixtures measured from mass flow rates through a single microtube. *Phys. Fluids*, 28(9):092001, 2016.

[17] C. Tantos, D. Valougeorgis, M. Pannuzzo, A. Frezzotti, and G. L. Morini. Conductive heat transfer in a rarefied polyatomic gas confined between coaxial cylinders. *Int. J. Heat Mass Transf.*, 79:378 – 389, 2014.

[18] W. M. Trott, J. N. Castañeda, J. R. Torczynski, M. A. Gallis, and D. J. Rader. An experimental assembly for precise measurement of thermal accommodation coefficients. *Rev. Sci. Instrum.*, 82:0355120, 2011.

[19] G. S. Springer. Heat transfer in rarefied gases. In T. F. Irvine and J. P. Harnett, editors, *Advanced in heat transfer*, pages 163–218. Academic, New York, 1971.

[20] F. S. Sherman. A survey of experimental results and methods for the transitional regime of rarefied gas dynamics. In J. A. Lauermann, editor, *Rarefied Gas Dynamic, Proc. 3rd Int. Symp. on Rarefied Gas Dynamics*, volume II, pages 228–260. Academic Press, New York, 1963.

[21] H. Yamaguchi, M. T. Ho, Y. Matsuda, T. Niimi, and I. Graur. Conductive heat transfer in a gas confined between two concentric spheres: From free-molecular to continuum flow regime. *Int. J. Heat Mass Transf.*, 108:1527–1534, 2017.

[22] G. A. Bird. *Molecular Gas Dynamics and the Direct Simulation of Gas Flows*. Clarendon Press, New York, 1994.

[23] Jr. J. R. Rumble, editor. *CRC Handbook of Chemistry and Physics, 98th Edition*. CRC Press, 2017.

[24] E A Mason and S C Saxena. Approximate formula for the thermal conductivity of gas mixtures. *Phys. Fluids*, 1(5):361–369, 1958.

[25] W. Cencek, M. Przybytek, J. Komasa, J. B. Mehl, B. Jeziorski, and K. Szalewicz. Effects of adiabatic, relativistic, and quantum electrodynamics interactions on the pair potential and thermophysical properties of helium. *J. Chem. Phys.*, 136(22):224303, 2012.

[26] E. Vogel, B. Jager, R. Hellmann, and E. Bich. Ab initio pair potential energy curve for the argon atom pair and thermophysical properties for the dilute argon gas. ii. thermophysical properties for low-density argon. *Mol. Phys.*, 108(24):3335–3352, 2010.

[27] F. Sharipov and V. J. Benites. Transport coefficients of helium-argon mixture based on ab initio potential. *J. Chem. Phys.*, 143(15):154104, 2015.

[28] J. Kestin, K. Knierim, E. A. Mason, B. Najafi, S. T. Ro, and M. Waldman. Equilibrium and transport properties of the noble gases and their mixtures at low density. *J. Phys. Chem. Ref. Data*, 13(1):229–303, 1984.

[29] M. T. Ho and I. Graur. Heat transfer through rarefied gas confined between two concentic spheres. *Int. J. Heat Mass Transf.*, 90:58–71, 2015.

[30] I. Amdur and L. A. Guildner. Thermal accommodation coefficients on gas-covered tungsten, nickel and platinum. *J. Am. Chem. Soc.*, 79(2):311–315, 1957.

[31] L. B. Thomas and F. Olmer. The accommodation coefficients of he, ne, a, h2, d2, o2, co2, and hg on platinum as a function of temperature. *J. Am. Chem. Soc.*, 65(6):1036–1043, 1943.

[32] S. Rezaeiravesh, R. Vinuesa, M. Liefvendahl, and P. Schlatter. Assessment of uncertainties in hot-wire anemometry and oil-film interferometry measurements for wall-bounded turbulent flows. *Eur. J. Mech. B. Fluids*, 72:57–73, 2018.

[33] F Sharipov. Data on the velocity slip and temperature jump on a gas-solid interface. *J. Phys. Chem. Ref. Data*, 40(2):023101, 2011.